Heliyon 10 (2024) e33240

Contents lists available at ScienceDirect

Heliyon

journal homepage: www.cell.com/heliyon

Research article

Effect of a topical traditional Chinese herbal medicine on skin microbiota in mouse model of atopic dermatitis

Bijun Zeng [a,b,c], Xuewei Liu [d], Yi Zhou [e], Gutao Cui [f], Lili An [f], Zhibo Yang [c,*]

[a] School of Traditional Chinese Medicine, Hunan University of Chinese Medicine, Changsha, 410208, China
[b] Hunan Engineering Technology Research Center for Medicinal and Functional Food, Hunan University of Chinese Medicine, Changsha, 410208, China
[c] Department of Dermatology, the Second Affiliated Hospital of Hunan University of Chinese Medicine, the Domestic First-class Discipline Construction Project of Chinese Medicine of Hunan University of Chinese Medicine, Changsha, 410005, China
[d] Department of Dermatology, the First Affiliated Hospital of Henan University of Chinese Medicine, Zhengzhou, 450000, China
[e] Department of Pharmacy, the Second Affiliated Hospital of Hunan University of Chinese Medicine, Changsha, Hunan, 410005, China
[f] Department of Medical Marketing, Hefei Yifan Biomedicine Med. Co., Ltd., Hefei, 230001, China

ARTICLE INFO

Keywords:
Chushi Zhiyang Ruangao (CSZYRG)
Atopic dermatitis (AD)
Inflammation
Skin microbiota
Dominant flora

ABSTRACT

This study aims to explore the impact of the herbal ointment Chushi Zhiyang Ruangao (CSZYRG) on the skin's microecological environment in a mouse model of atopic dermatitis (AD) and to understand the underlying mechanisms involved. The AD model was established in C57 mice using calpolitol (a hypocalcemic analog of vitamin D3; MC903). Medication-free matrix ointment, CSZYRG, and mometasone furoate cream (positive control group) were applied to the injured areas. The skin lesions of AD model mice were photographed. Skin lesions were applied for the hematoxylin and eosin (H&E) staining to observe any pathological changes. Serum immunoglobulin IgE was detected by enzyme-linked immunosorbent assay (ELISA). The changes in the expression of inflammation-related factors TNF-α, IL-1β, and IL-6 in mice were detected using ELISA and qRT-PCR. Skin microflora samples were taken for 16S rDNA sequencing and analyzed for changes in the skin flora diversity, abundance, and dominant flora in mice. It was concluded that CSZYRG effectively alleviates skin lesions, serum IgE, and levels of TNF-α, IL-1β, and IL-6 in AD model mice. However, CSZYRG did not affect the skin microbial diversity of AD model mice but could exert an effect on the skin microbial community in AD mice and the relative abundance of the dominant microflora. CSZYRG may play a therapeutic role in AD by affecting the skin microbial community and relative abundance of dominant microflora in AD mice.

1. Introduction

Atopic dermatitis (AD) or atopic eczema is a chronic, recurrent, and remission inflammatory dermatological disorder. The disease is mainly characterized by scaly, itchy, erythematous lesions on the curved surface of the skin [1,2]. AD affects up to 12 % of children and 7.2 % of adults [3]. AD is caused by a complex interplay of immune disorders, epidermal gene mutations, and environmental factors. These factors damage the epidermis and lead to intensely itchy skin damage. Sustained scratching triggers a self-sustaining itch-scratch

* Corresponding author. Department of Dermatology, the Second Affiliated Hospital of Hunan University of Chinese Medicine, the Domestic First-class Discipline Construction Project of Chinese Medicine of Hunan University of Chinese Medicine, Changsha, Hunan, 410005, China.
E-mail address: dr_yangzhibo@163.com (Z. Yang).

https://doi.org/10.1016/j.heliyon.2024.e33240
Received 2 August 2023; Received in revised form 20 May 2024; Accepted 17 June 2024
Available online 18 June 2024

cycle, thereby significantly impacting quality of life. AD usually begins in childhood, with 60 % of patients developing AD by the age of 1 year and 90 % by the age of 5 years [4]. Children with AD are more likely to suffer from food and environmental allergies, asthma, and allergic rhinitis than children without AD [5]. Patients with AD are also more likely to suffer from ear infections, streptococcal pharyngitis, and urinary tract infections [6].

AD symptoms can be divided into the dampness of spleen deficiency syndrome, dampness and heat accumulation syndrome, blood deficiency, and wind dryness syndrome. Traditional Chinese Medicine (TCM) treats AD from a holistic perspective and believes that AD is caused by dampness-heat and that the treatment of eczema should focus on regulating the spleen and stomach. The basic treatment plan is divided into dispelling dampness and mitigating toxins, invigorating the spleen to remove dampness, harmonizing the spleen and stomach, nourishing blood, and dispelling wind. In traditional TCM, Qu Feng (dispelling wind) targets the expulsion of the 'wind,' an external pathogen in TCM believed to cause symptoms like moving pains, itching, and tremors. Known for their dispersing properties, Qu Feng treatments relieve these kinds of symptoms by relieving 'wind' from the muscles, joints, meridians, and skin. In many Asian countries such as China, Japan, Korea, India, and Iran, TCM is used in the clinical field of AD for its excellent efficacy and safety. For example, some TCM formulas could attenuate AD-related cells' contribution to AD progression through antioxidant activity [7]. In addition, TCM may affect the structure of developing dendritic cells (DCs) because they lose their typical dendritic morphology and reduce the expression of CD1a and the low-affinity IgE receptor CD23 [8].

The herbal ointment, CSZYRG is composed of several Chinese herbs, such as common *Cnidium* fruit, *Coptis Chinensis*, *Phellodendri Chinensis Cortex*, *Dictamni Cortex*, *Sophorae Flavescentis Radix*, giant knotweed rhizome, *Violae Herba*, *Kochiae Fructus*, *Herba Polygoni Avicularis*, *Herba Artemisiae Scopariae*, *Atractlodis Rhizoma*, *ZanthoxμLi Pericarpium*, *Borneolum Syntheticum*, etc. It clears heat, removes dampness, dispels wind, and relieves itching. According to < Guidelines for Clinical Application of Proprietary Traditional Chinese Medicines in the Treatment of Eczema (2020) > [9], single topical or oral CSZYRG can effectively treat eczema. It can reduce skin lesions, relieve itching, reduce eczema recurrence, and complement conventional Western medicine as an alternative therapy [10,11]. CSZYRG combination with conventional Western medicine can boost the therapeutic effect, exerting a synergistic interaction effect on conventional Western medicine [12,13]. In terms of mechanism, various active components of CSZYRG have been confirmed to have alleviating effects on the clinical symptoms of AD through different pathways [14–16].

The skin microbiota can be involved in the regulation of inborn and adaptive immune responses [17]. Reduced microbial diversity in AD patients correlates with disease severity and increased colonization by pathogenic bacteria (such as *Staphylococcus aureus*) [18]. For example, early clinical studies concluded that the topical application of commensal bacteria (e.g., human staphylococci [19] or roseomonas mucosa [20]) reduced AD severity.

The effects of CSZYRG treatment on the skin microbiota of AD model mice were investigated in this study. Furthermore, the study explored and elucidated the mechanism of CSZYRG treatment for AD from the perspective of skin microecology to furnish fresh concepts for the clinical treatment of AD.

2. Materials and methods

2.1. CSZYRG composition and preparation

CSZYRG was procured from Hefei Yifan Bio-Pharmaceutical Co., Ltd. The cream contained 13 herbs (Table 1) and cream vehicle (sodium lauryl sulfate, glycerin, petrolatum, and cetyl Alcohol). All the herbs were prepared in proportion by soaking in 16 times their weight in pure water and were then extracted thrice by refluxing for 1 h. This solution was then filtered, and the filtrate was concentrated into a thick paste with a relative density of 1.10–1.20 (60 °C). The solution was subsequently mixed with a cream vehicle and stirred until condensed.

2.2. Quality analysis of CSZYRG by high-performance liquid chromatography and mass spectrometry (HPLC-MS)

HPLC was performed on the Agilent 1200 Series Gradient HPLC system (Agilent, CA, USA). A Hypersil GOLD C18 column (5 μm, 4.6

Table 1
Composition of CSZYRG (10 g cream).

Herb name	Chinese Name	Raw herb Weight
Common Cnidium Fruit.	Shechuangzi	1.67 g
Coptis chinensis Franch.	Huanglian	0.37 g
Coptis chinensis Franch.	Huangbo	0.37 g
Dictamnus dasycarpus Turcz.	Baixianpi	0.56 g
Sophorae flavescentis radix.	Kushen	0.56 g
Reynoutria japonica Houtt.	Huzhang	0.74 g
Viola yedoensis Makino.	Zihuadiding	0.74 g
Kochia scoparia (L.) Schrad.	Difuzi	0.93 g
Polygonum aviculare (L.) Polygonaceae	Bianxu	0.56 g
Artemisia capillaris Thunb.	Yinchen	0.56 g
Atractylodes lancea (Thunb.) Dc.	Cangzhu	0.37 g
Zanthoxylum bungeanum Maxim.	Huajiao	0.19 g
Borneolum syntheticum	Bingpian	0.15 g

mm × 250 mm) was used for all analyses at 35 °C. The mobile phase was composed of acetonitrile (A), and 0.05 % formic acid (v/v) (B). The flow rate was 1 mL/min with 65 min of gradient elution: 0–35 min, 5–30 % A; 35–44 min, 30–40 % A; 45–60 min, 40–90 % A; 60–65 min, 90 % A. The MS analysis was performed on Agilent 6120 Single Quadrupole LC/MS System (Agilent) with an electrospray ionization source in both positive and negative ionization modes with a capillary voltage of 3000 V, gas temperature of 350 °C and nebulizer at 35 psi. The chromatogram HPLC-MS of CSZYRG in positive and negative ion modes is shown in Fig. S1.

2.3. AD mouse molding

Female C57 mice (six weeks old), n = 25; mice were acclimatized and fed for one week and then molded. All procedures were approved by the Ethics Committee of Hunan Experimental Animal Center (Approval number: IACUC-2021(5)070).

MC903 (calpolitol, a hypocalcemic analog of vitamin D3, #S82049, Yuanye Bio, Shanghai, China) was applied topically to establish the AD mice model. MC903 (4 nmol, dissolved in DMSO) was applied topically to the back of the ears in the AD mouse model group, the vehicle group, the CSZYRG treatment group, and the positive control group. MC903 (4 nmol) was applied topically daily for 10 days from day 7 to day 16. The normal control group was given 10 μL of DMSO on the back of the ears as solvent control. After 24 h of final molding, observation of lesion morphology with bloody crusts, scales, brown erythema, pathological morphology hyperkeratosis, acanthosis, and inflammatory cell infiltration was indicated as successful molding.

The mice were grouped into (1) blank control group, (2) model group, (3) model + vehicle group, (4) model + (positive control, mometasone furoate cream) and (5) model + CSZYRG; 5 mice in each group. At day 17, cream substrate, mormisone furoate cream (Shanghai Xinya Pharmaceutical, China) and CSZYRG were applied to the model + cream vehicle group, model + positive control group and model + CSZYRG group respectively; once daily for 7 days from day 17–23.

2.4. Sample collection

Twenty-four hours after the last administration, the mice were anesthetized with 1 % sodium pentobarbital (50 mg/kg). Blood samples were collected from the hearts of the mice and left at room temperature for 30 min. Afterward, the serum was centrifuged at 3000r/min at 4 °C for 15 min. The ears were divided into three parts. One part of the skin tissue was fixed with 4 % paraformaldehyde and sent to the pathology laboratory for H&E staining. The other two parts of the skin were stored in a −80 °C refrigerator pending 16s rDNA sequencing, and qRT-PCR analysis.

2.5. Eczema area and severity index score

The Eczema Area and Severity Index (EASI) score is widely used in new medicine validation of eczema [21,22]. EASI is a score of four clinical manifestations: erythema (E), sclerosis (edema)/papula (I), epidermal exfoliation (Ex), and lichenification (L). The severity of the four manifestations was scored on a scale of 0–3: 0.5 – none/mild; 1 – mild; 1.5 – mild/moderate; 2 – moderate; 2.5 – moderate/severe; and 3 – severe.

2.6. Hematoxylin and eosin (H&E) staining

Paraffin sections were dewaxed in xylene, rehydrated in gradient concentration of alcohol, washed in PBS, and immersed in H&E staining solution for 10 min. The slide was immersed in dilute hydrochloric acid alcohol for 5 s after washing with tap water, in light ammonia for 5 min after tap water washing, and in eosin for 10 min after tap water washing. The slide was immersed in 70 %, 80 % and 90 % alcohol once each in turn for 1 min after tap water washing, in 95 % alcohol twice for 1 min each, then in anhydrous ethanol three times for 1 min each, and in xylene three times for 1 min each. Finally, the slide was sealed with neutral resin.

2.7. qRT-PCR

Tissue samples were collected. Total RNA was extracted using TRIZOL (Invitrogen, Carlsbad, CA, USA). Reverse transcription was performed using a reverse transcription kit (TaKaRa, Tokyo, Japan), and all operations were performed according to the instructions of the reverse transcription kit. Gene expression was detected using a LightCycler 480 instrument (Roche Diagnostics, Switzerland) and

Table 2
qRT-PCR primer list.

Primer name		Sequence (5′-3′)
TNF-α	Forward	CCCTCACACTCAGATCATCTTCT
	Reverse	GCTACGACGTGGGCTACAG
IL-1β	Forward	CTGTGACTCATGGGATGATGATG
	Reverse	CGGAGCCTGTAGTGCAGTTG
IL-6	Forward	TAGTCCTTCCTACCCCAATTTCC
	Reverse	TTGGTCCTTAGCCACTCCTTC
GAPDH	Forward	AGGTCGGTGTGAACGGATTTG
	Reverse	TGTAGACCATGTAGTTGAGGTCA

qRT-PCR kit, and reaction conditions were performed according to the operating instructions of the qRT-PCR kit (SYBR Green Mix, Roche Diagnostics). The thermal cycling parameters were: 95 °C for 10s, then 95 °C for 5s, 60 °C for 10s, 72 °C for 10s, for a total of 45 cycles; and finally 72 °C for 5min. qRT-PCR was set up with 3 replicates for each reaction. GAPDH was used as the internal reference. Data were analyzed by the $2^{-\Delta\Delta Ct}$ method. The amplification primer sequences for each gene and its internal reference are detailed in Table 2.

2.8. Enzyme-linked immunosorbent assay (ELISA)

The content of IgE (RX202737 M, Ruixinbio, Quanzhou, China), TNF-α (RX202412 M, Ruixinbio), IL-6 (RX203049 M, Ruixinbio), and IL-1β (RX203063 M) in mice serum of each group was detected by ELISA kit, and all operations were performed strictly according to the ELISA kit instructions. The optical density (OD) of each well was determined at 450 nm wavelength using a multifunctional microplate reader (Bio-rad, USA).

2.9. Microflora diversity sequencing analysis (16S rDNA sequencing)

Universal primers were designed using gene segments of the bacterial 16SrDNA conserved V3V4 region. PCR amplification was performed using forward primer 341F: CTACGGGNGGCWGCAG and reverse primer 805R: GACTACHVGGGTWTCTAATCC. The V3V4 region of the 16S rRNA gene was sequenced using paired-end sequencing on the Illumina NovaSeq system (MiSeq, version 3). The raw

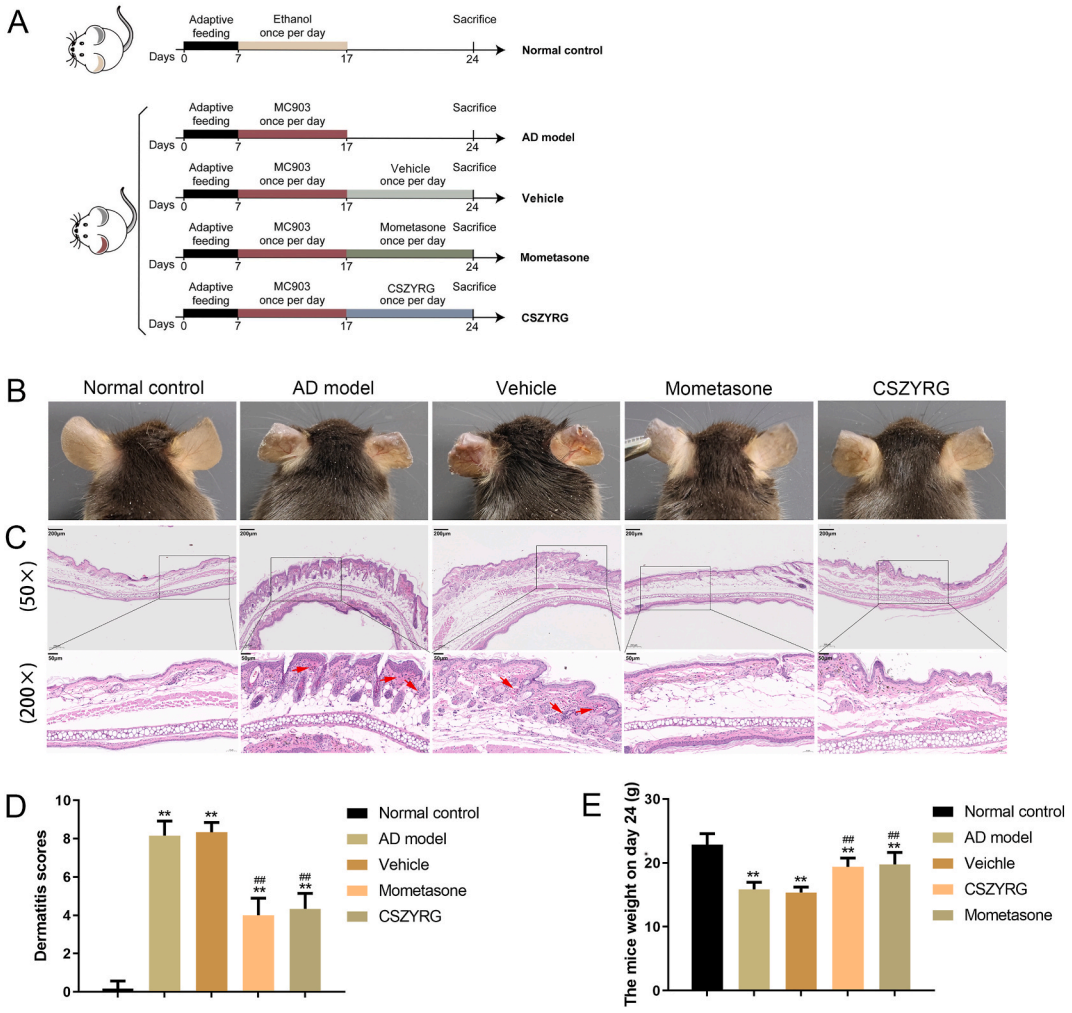

Fig. 1. CSZYRG alleviates symptoms in AD mice at macroscopic and microscopic levels. (A) Schematic diagram of eczema mouse model construction and grouping. (B) Photographs of mouse ears skin lesion; (C) HE staining of skin lesions to observe pathological changes. 50× magnification scale bar is200 μm; 200× magnification scale bar is 50 μm. (D) The Eczema Area and Severity Index (EASI) scores of skin lesions were evaluated. (E) Comparison of mice body weights in each group. $^{**}P < 0.01$, compared with the normal control group. $\#\#P < 0.01$, compared with the Vehicle group.

data were pre-processed and analyzed using QIIME software (version 1.9). Clean tags were obtained by filtering low-quality reads with UCHIME, removing barcode and primer sequences from both ends of tags, and removing chimeric sequences. Pairs of clean tags were pieced together into a sequence according to the overlapping relationship between PE data. According to the similarity of 0.97, Operational Taxonomic Units (OTUs) of species classification were clustered using QIIME software (2020.2). The abundance of information on each OTU in each sample was counted. The abundance of OTUs can initially reflect the abundance of species in the samples.

2.10. Alpha and beta diversity index

Alpha diversity is an indicator that responds to richness, diversity, and homogeneity. SOB (Observed species: counts the total number of unique species detected), Chao (Abundance-based coverage estimator emphasizing the contribution of rare species), ACE (Abundance-based coverage estimator accounting for both rare and abundant species), Shannon (a combined measure of richness and evenness, with higher values indicating greater diversity), Simpson (Represents the probability that two randomly selected individuals belong to the same species, with lower values suggesting higher diversity), and the goods-coverage index (Estimates the sampling completeness, with values near 1 indicating extensive species detection) were used in this study. Beta diversity is the rate of species turnover along an environmental gradient or the similarity of species composition between different communities varying along the environmental gradient. It is usually analyzed using principal component analysis (PCA) and nonmetric multidimensional scaling

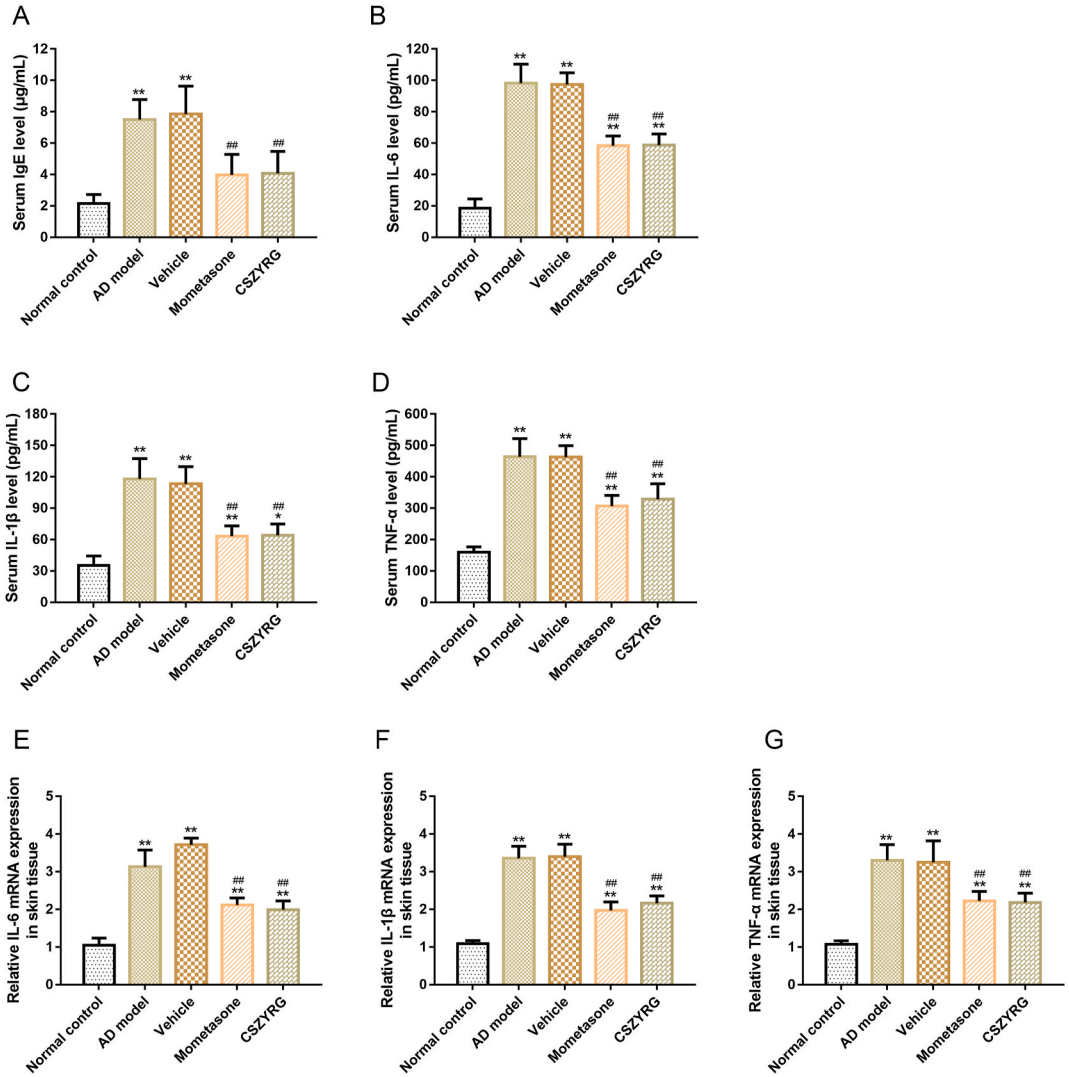

Fig. 2. CSZYRG alleviates the inflammation level of AD mice. (A) Serum IgE level; (B) Serum IL-6 level; (C) Serum IL-1β level; (D) Serum TNF-α level; (E–G) The relative mRNA expression of IL-6, IL-1β and TNF-α in ear skin tissues. $^{**}P < 0.01$, compared with the normal control group. $\#\#P < 0.01$, compared with the Vehicle group.

(NMDS). PCA is utilized to reduce the dimensionality of the complex dataset, summarizing the variation in microbial community composition across different samples into principal components that can be more easily visualized and interpreted. NMDS is an ordination method that simplifies the complexity of high-dimensional data into a two-dimensional space, aiding in the visualization of the dissimilarity among samples.

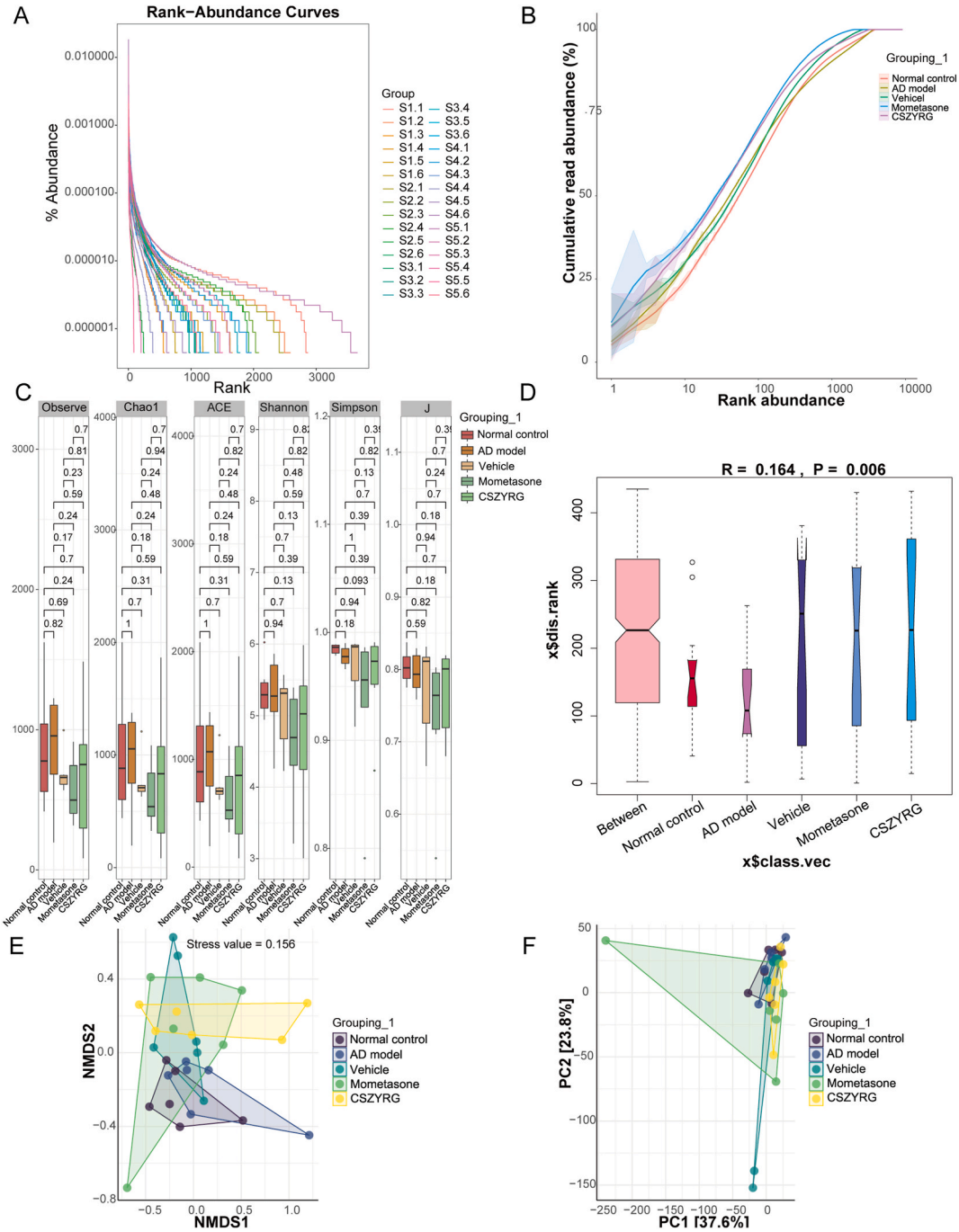

Fig. 3. Quality control analysis of 16S sequencing data of skin microbiota. (A–B) Dilution curves showing the species composition (length of the horizontal axis; the wider the curve, the richer the species composition) and homogeneity (reflected by the shape of the vertical axis of the curve; the flatter the curve, the more homogeneous the species composition in the sample) of the skin microbiota of each group of study subjects. (C) Alpha diversity analysis. (D) Anosim differential analysis. (E–F) Beta diversity analysis parameters NMDS and PCA are used to evaluate inter-group differences in microflora.

2.11. Data analysis

Experimental data from individual experiments were presented as the mean ± standard deviation (SD). One-way ANOVA with post-hoc Tukey HSD test was used for multiple comparisons. The difference between the two groups was analyzed by student t-test. The difference among more than two groups was analyzed by the Kruskal–Wallis test. $P < 0.05$ denotes a statistically significant difference.

3. Result

3.1. CSZYRG alleviates symptoms in AD mice at macroscopic and microscopic levels

Firstly, the AD mice model was constructed, and the corresponding treatment was given to investigate the effect of CSZYRG on AD. The schematic diagram of AD mice model construction, grouping, and corresponding treatment is shown in Fig. 1A. The morphological and histological changes at the lesion site are shown in Fig. 1B and C. The epidermis and dermis of the normal group were intact in structure and normal in thickness. Hyperkeratosis, lamellar cuticle, acanthosis, and heavy dermal edema were seen in the AD and Vehicle groups, with lymphocyte and eosinophil infiltration (red arrows indicate infiltration). The pathological morphology was consistent with chronic eczema model morphology, indicating successful membrane building and the lack of therapeutic effect of stromal ointment. The hyperkeratotic condition, edema, and inflammatory cell infiltration degree were significantly reduced in the CSZYRG and Mometasone groups compared with the AD group, indicating that the pathological morphology was significantly improved in the CSZYRG and Mometasone groups. The skin lesion score can reflect the local skin lesion. The score is directly proportional to the severity of the damage. The body weight can reflect the eating and emotional state of the mice to some extent. The results of Fig. 1D and E are consistent with HE results. The skin lesion score was significantly upregulated, and the body weight was significantly decreased in the modeling groups compared with the Control group. The AD and Vehicle groups had the highest skin lesion score and lowest body weight, followed by the CSZYRG and Mometasone groups. These findings indicate that the modeling was successful, and the skin lesions and emotional status of the mice were significantly improved in the CSZYRG and Mometasone groups. These results show that CSZYRG is effective in treating the AD mice model.

3.2. CSZYRG reduces inflammation levels in AD mice

The expression of immunoglobulin IgE and inflammation-related factors TNF-α, IL-1β, and IL-6 in each group of mice serum was detected using ELISA. Serum IgE was significantly upregulated in all groups of mice models compared to the normal control group, with the highest in the AD and Vehicle groups. In contrast, serum IgE was decreased in the CSZYRG and Mometasone treatment groups compared with the AD group (Fig. 2A). The changes in TNF-α, IL-1β, and IL-6 expression were consistent with the trend of serum IgE (Fig. 2B–D). The changes in mRNA expression of TNF-α, IL-1β, and IL-6 in ear skin tissues were further detected using qRT-PCR. The mRNA expression of TNF-α, IL-1β, and IL-6 in Fig. 2E–G was consistent with the serum ELISA trend which was increased in the AD model and reduced by CSZYRG and Mometasone treatments. The above results indicate that CSZYRG can reduce the inflammatory response in AD mice.

3.3. Quality control analysis of 16S sequencing data of skin microbiota

Sample collection was conducted using skin cotton swabs from mice in each experimental group (n = 6), and changes in skin microbiota diversity were analyzed using 16rRNA gene sequencing. The abundance of species in each group of samples was first analyzed using a substance accumulation curve graph. Group naming: Normal control, AD, Vehicle, Mometasone, and CSZYRG. Species composition was abundant in all groups of samples, and the homogeneity of species composition was high enough to be used for subsequent analysis (Fig. 3A). Sequencing volumes were evaluated by dilution curves (abundance curves) to determine whether they were sufficient to cover the species abundance in the sample. The curves of all 5 groups of samples tended to be flat, indicating that the sequencing depth of this experiment covered all species in the samples (Fig. 3B). The results of the Alpha diversity analysis are shown in Fig. 3C. Observed species, Chao1, and ACE were used to reflect the number of species in the community. Shannon, Simpson, and J were used to evaluate the microbial diversity in the samples. The results showed no inter-group difference in the diversity of skin microbiota in each mouse group. Anosim variance analysis is shown in Fig. 3D ($R = 0.164$, $P = 0.006$); it indicated that the between-group differences were greater than the within-group differences. Mouse skin communities were affected by AD modeling and by different medicine treatments. Beta diversity analysis can reflect inter-group differences in microflora. Fig. 3E shows NMDS analysis, and Fig. 3F shows PCA. The results were consistent with the results of the Anosim difference analysis, suggesting inter-group differences in skin microbiota.

3.4. Comparison of absolute OTU abundance among mice groups

The absolute OTU abundance in the normal control and AD groups had about 37 % consistency, sharing 1447 overlapping OTUs (Fig. 4A). The absolute OTU abundance of the AD group with Vehicle had about 32 % consistency, sharing 1212 overlapping OTUs (Fig. 4B). The absolute OTU abundance in the AD and Mometasone groups had about 28 % consistency, sharing 1063 overlapping OTUs (Fig. 4C). The absolute OTU abundance in the AD and CSZYRG groups had about 55 % consistency, sharing 1259 overlapping OTUs (Fig. 4D). The absolute OTU abundance in the Vehicle and CSZYRG groups had about 45 % consistency, sharing 1340

overlapping OTUs (Fig. 4E). The absolute OTU abundance in the Mometasone and CSZYRG groups had about 38 % consistency, sharing 1265 overlapping OTUs (Fig. 4F).

3.5. Comparison of the dominant microflora in mice skins

Given that there was a degree of consistency in the absolute OTU abundance of mice's skin between treatment groups, an analysis was conducted to determine how comparable the dominant species composition was across these groups. Fig. 5 shows that the composition of the main dominant microflora groups was similar in different groups, including *Muribaculaceae*, *Lactobacillus*, *Akkermansia*, *Lachnospiraceae_NK4A136_group*, *Bacteroides*, *Alistipes*, *Staphylococcus*, *Lawsonella*, *Helicobacter*, *Escherichia-Shigella*, *Alloprevotella*, *Rikenellaceae_RC9_gut_group*, *f_Rikenellaceae_ASV_15*, *Parabacteroides*, *Prevotellaceae_UCG-001*, *Clostridia_UCG-014*, *Dubosiella*, *Candidatus_Saccharimonas* and *Chloroplast*.

3.6. Comparison of the relative abundance of the dominant microbiota species in mice skins

Next, the differences in the relative abundance of the dominant microbiota species in each group were further analyzed. The Kruskal-Wallis test suggests that the relative abundance of *Lawsonella* and *Chloroplast* are different among the five groups (Table 3). Pairwise comparisons of relative microbial abundance between groups were performed. The relative abundance of *Helicobacter* *Lachnospiraceae_NK4A136_group* seems to be lower in the AD group while *Clostridia_UCG-014*, *Dubosiella*, *Staphylococcus*, *Chloroplast* and *Lactobacillus* tend to be higher in the AD group compared to the normal control group, while the difference was not significant

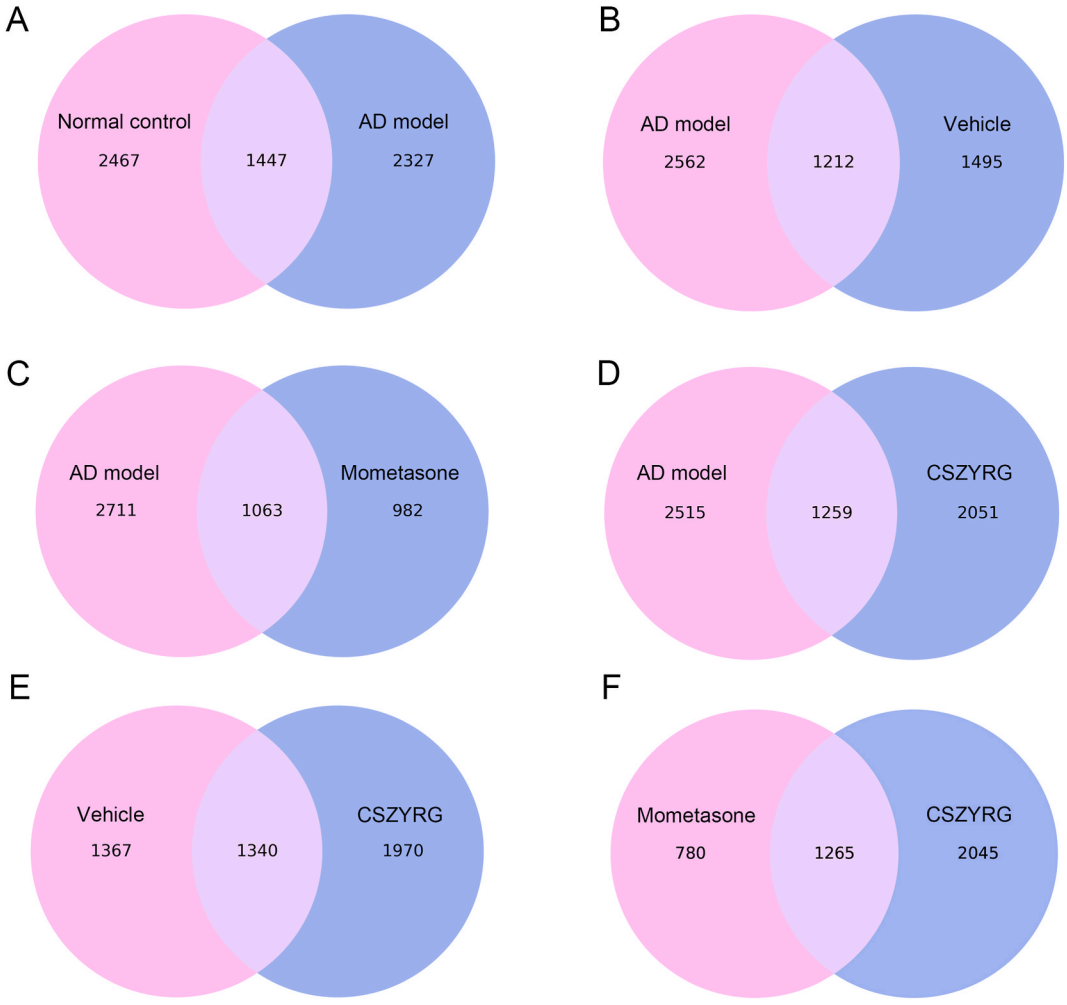

Fig. 4. Comparison of Operational Taxonomic Unit (OTU) abundance among mice groups (A) Comparison of absolute OTU abundance in the normal control and AD groups. (B) Comparison of absolute OTU abundance in the AD group and Vehicle. (C) Comparison of absolute OTU abundance in the AD and Mometasone groups. (D) Comparison of absolute OTU abundance in the AD and CSZYRG groups. (E) Comparison of absolute OTU abundance in the Vehicle and CSZYRG groups.

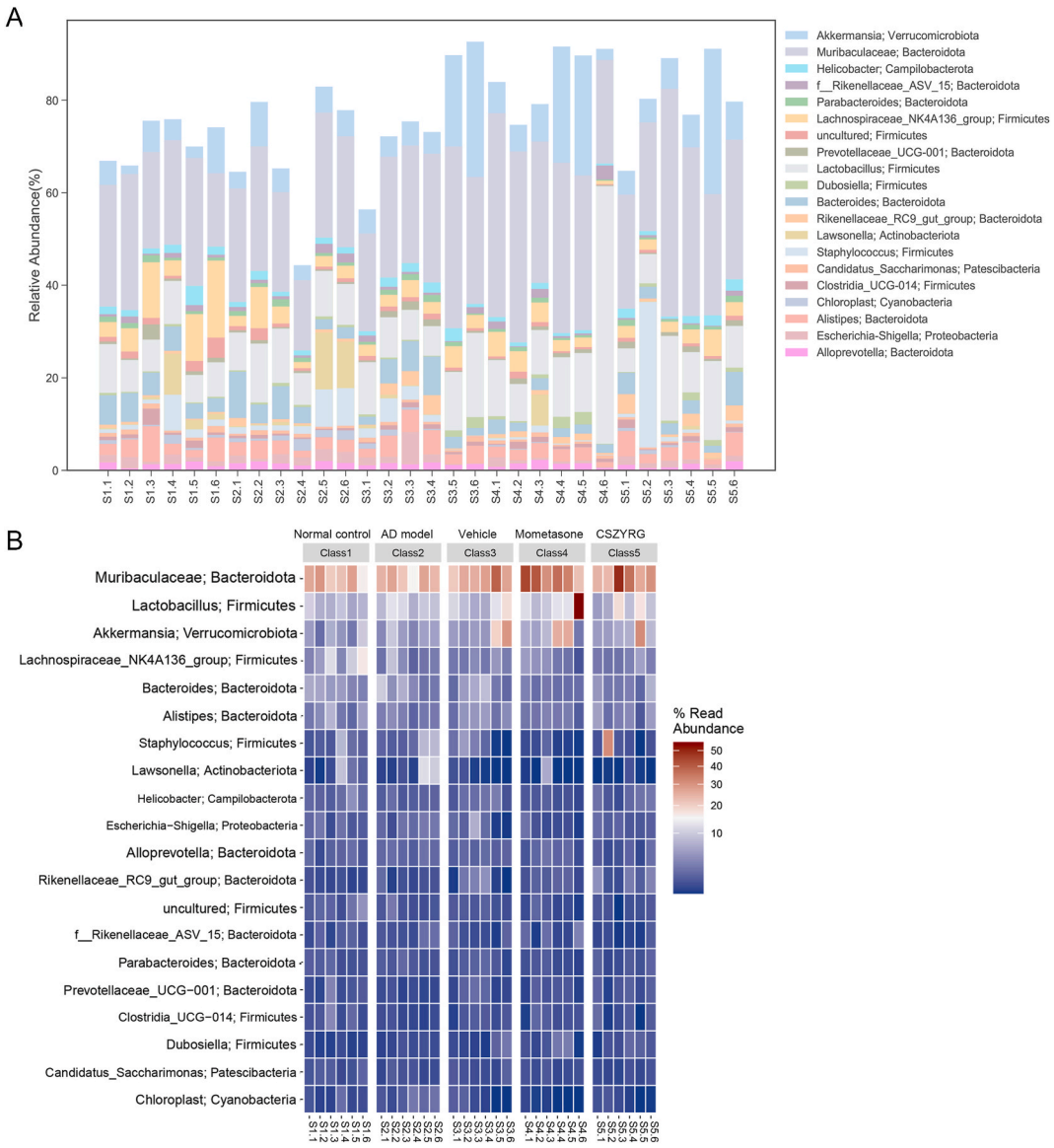

Fig. 5. Comparison of the relative abundance of the dominant microflora in mice skins. The top 20 most abundant microflora groups in the skin microecology of mice in each treatment group are shown respectively in the bar graph (A) and heat map (B). The similarity of the dominant species composition of different groups was observed.

(Fig. 6A). The relative abundance of *Chloroplast* was significantly higher in the AD group compared to the Vehicle group ($p < 0.05$, Fig. 6B). The relative abundance of *Muribaculaceae* was lower in the AD group compared to the Mometasone group, while the relative abundance of *Helicobacter*, *Chloroplast* and *Escherichia-Shigella* was higher in the AD group ($p < 0.05$, Fig. 6C). The relative abundance of *Prevotellaceae_UCG-001* was lower in the AD group compared to the CSZYRG group, while the relative abundance of *Chloroplast* was higher in the AD groups ($p < 0.05$, Fig. 7A). The relative abundance of microbiota between the CSZYRG and Vehicle groups saw no significant differences (Fig. 7B). Compared to the Mometasone group, the relative abundance of *Helicobacter* was higher in the CSZYRG group ($p < 0.05$, Fig. 7C). The differences in the relative abundance of the dominant skin microflora of mice in each treatment group are listed in Table 4. As the result showed, the AD model induced the upregulated *Staphylococcus* relative abundance and down-regulated the relative abundance of *Muribaculaceae*, *Helicobacter*, *Lachnospiraceae_NK4A136_group*, *Prevotellaceae_UCG-001*, and *Clostridia_UCG-014* were reversed by CSZYRG treatment, though the difference was not significant.

4. Discussion

The epithelium of human skin is home to large colonies of microorganisms. Many of the roles played by the microbiota on our

Table 3
Comparison of relative median abundance of the skin dominant microbiota among five groups.

Genus	Normal control(%)	AD model(%)	Vehicle(%)	Mometasone(%)	CSZYRG(%)	p.value
Akkermansia	4.856493	5.375816	5.210812	7.434753	6.827621	0.411858
Muribaculaceae	24.44742	24.24574	26.77899	35.09084	28.1914	0.069384
Helicobacter	1.707893	1.209536	1.940737	0.77236	1.796308	0.055697
f_Rikenellaceae_ASV_15	0.808986	0.806511	0.58442	1.006965	0.356155	0.151797
Parabacteroides	0.90191	0.882202	0.985477	0.564219	0.816006	0.363037
Lachnospiraceae_NK4A136_group	7.568992	2.502032	2.683013	3.317291	2.746094	0.101850
uncultured	1.460356	0.785831	0.942071	0.471844	0.66465	0.063342
Prevotellaceae_UCG-001	0.663962	0.449009	0.881835	0.789724	1.024862	0.549582
Lactobacillus	7.184937	9.328359	9.989584	12.4466	8.858459	0.253183
Dubosiella	0.274938	0.496699	0.441463	0.756874	0.833122	0.240392
Bacteroides	5.067963	3.786806	3.867481	1.91837	2.718058	0.138757
Rikenellaceae_RC9_gut_group	0.472926	0.655171	1.349459	1.118307	1.848247	0.221375
Lawsonella	0.882332	0.480035	0.170383	0.056825	0.100708	0.033773*
Staphylococcus	1.210455	1.526605	1.764724	0.368127	0.726144	0.077977
Candidatus_Saccharimonas	0.923015	0.591421	0.644861	0.578299	0.474069	0.227442
Clostridia_UCG-014	0.786279	0.437865	0.899427	0.722989	0.734703	0.450790
Chloroplast	0.493187	1.30652	0.387331	0.11285	0.341075	0.010672**
Alistipes	3.076329	2.740168	4.177432	2.449164	3.269593	0.615816
Escherichia-Shigella	1.326727	1.895181	1.535926	0.561795	1.121063	0.198507
Alloprevotella	1.34895	1.586904	1.352515	1.467399	0.930672	0.369490

*p < 0.05, **p < 0.01.

bodies and the effects of dysbiosis are still unclear, despite growing evidence that they are crucial for human health and disease. The variety and skin site specificity of human microbial communities have been demonstrated by studies on skin microbiota, with varying microbial community compositions found in distinct skin surface locations [23,24]. The skin has the most diverse microbial communities in the body, with more than 1000 different bacteria from 19 different phyla [25,26]. A study of healthy adult volunteers showed that the skin microbiome is relatively stable over months to years and that different individuals have individually differentiated skin microbiota [27].

In this study, CSZYRG was effective in alleviating AD clinical manifestations compared to the Vehicle group and could reduce skin lesions and inflammation effectively, consistent with previous studies [28,29]. In further microbial community diversity sequencing analysis, the results show that CSZYRG has no effect on AD mice's skin microbial diversity but influences the community and abundance of dominant microflora in AD skin. The composition of the main dominant groups was similar in different groups, mainly *Muribaculaceae*, *Lactobacillus*, *Akkermansia*, *Lachnospiraceae_NK4A136_group*, *Bacteroides, Alistipes*, *Staphylococcus, Lawsonella*, *Helicobacter*, *Escherichia-Shigella*, *Alloprevotella*, *Rikenellaceae_RC9_gut_group*, *f_Rikenellaceae_ASV_15*, *Parabacteroides, Prevotellaceae_UCG-001*, *Clostridia_UCG-014*, *Dubosiella*, *Candidatus_Saccharimonas* and *Chloroplast*. However, the relative abundance of the dominant microflora was different across various treatment groups. Compared with the AD group, the relative abundance of *Prevotellaceae_UCG-001* was elevated in the CSZYRG group, whereas the relative abundance of *f_Rikenellaceae_ASV_15* and *Chloroplast* was decreased in the CSZYRG group. Compared to the Mometasone group, the relative abundance of *Helicobacter* was increased. In a study focusing on the effects of topical emollient therapy with sunflower seed oil on the skin microbiota of young children with severe acute malnutrition, *Prevotellaceae* were the most differentially affected by emollient treatment; several genera within this family became more abundant in the emollient group than in the controls across several skin sites [30]. The gut *Rikenellaceae* has been reported to be positively correlated with psoriasis-like pathological characteristics and negatively correlated with propionate levels [31]. Gut Abundance of *Rikenellaceae* has also been reported downregulated in chronic spontaneous urticaria [32] and negatively correlated with pro-inflammatory cytokines levels in ulcerative colitis [33]. CSZYRG-treated mice exhibited a lower abundance of *f_Rikenellaceae_ASV_15* in the AD mice's skin, while, mometasone therapy increased its abundance without statistical difference. Regarding *Helicobacter*, a relationship between gut *H. pylori* infection and chronic idiopathic urticaria, psoriasis, and atopic dermatitis has been reported [34,35]. Treatment of infection demonstrated by a reduction in *C-urea* breath test and anti-*H. pylori* antibody titers resulted in partial improvement of clinical symptoms in patients with atopic dermatitis [34]. However, in the AD mouse model, the *Helicobacter* infection alleviated AD manifestations by inducing the amplification of $CD4^{+}$CD25+Foxp3+Treg cells in the peripheral blood [36]. Interestingly, in the present study, mometasone decreased the dermal *Helicobacter* abundance in AD mice. CSZYRG exhibited an opposite effect on it, although the difference was not statistically significant. These results suggested that CSZYRG and mometasone may exert beneficial effects on AD mice by altering different dermal bacteria species. In addition, the trends that differ from the literature suggest that microbiota species may exhibit varied functions across different anatomical locations or diseases [37].

Besides, other species also saw trends of altered relative abundance. The opportunistic pathogen *Staphylococcus aureus* massively colonizes the lesional and non-lesional skin of people with atopic dermatitis (AD) [38]. In the present study, the pathogen *Staphylococcus*'s relative abundance was increased in AD mouse skin which was reduced by CSZYRG and mometasome treatment. Similarly, Liu et al. [39] also found the reduction of *Staphylococcus aureus* in skin microbiota of AD patients after topical mometasone and mupirocin administration. *Muribaculaceae* was sequenced and named in 2019 by Ilias Lagkouvardos and others [40]. Metformin can improve liver injury by upregulating *Muribaculaceae* to reduce colonic barrier dysfunction in septic-aged mice [41]. In a DSS-induced ulcerative colitis model, *Pulsatilla chinensis* saponins exerted anti-ulcerative colitis activity, possibly through the increase in beneficial

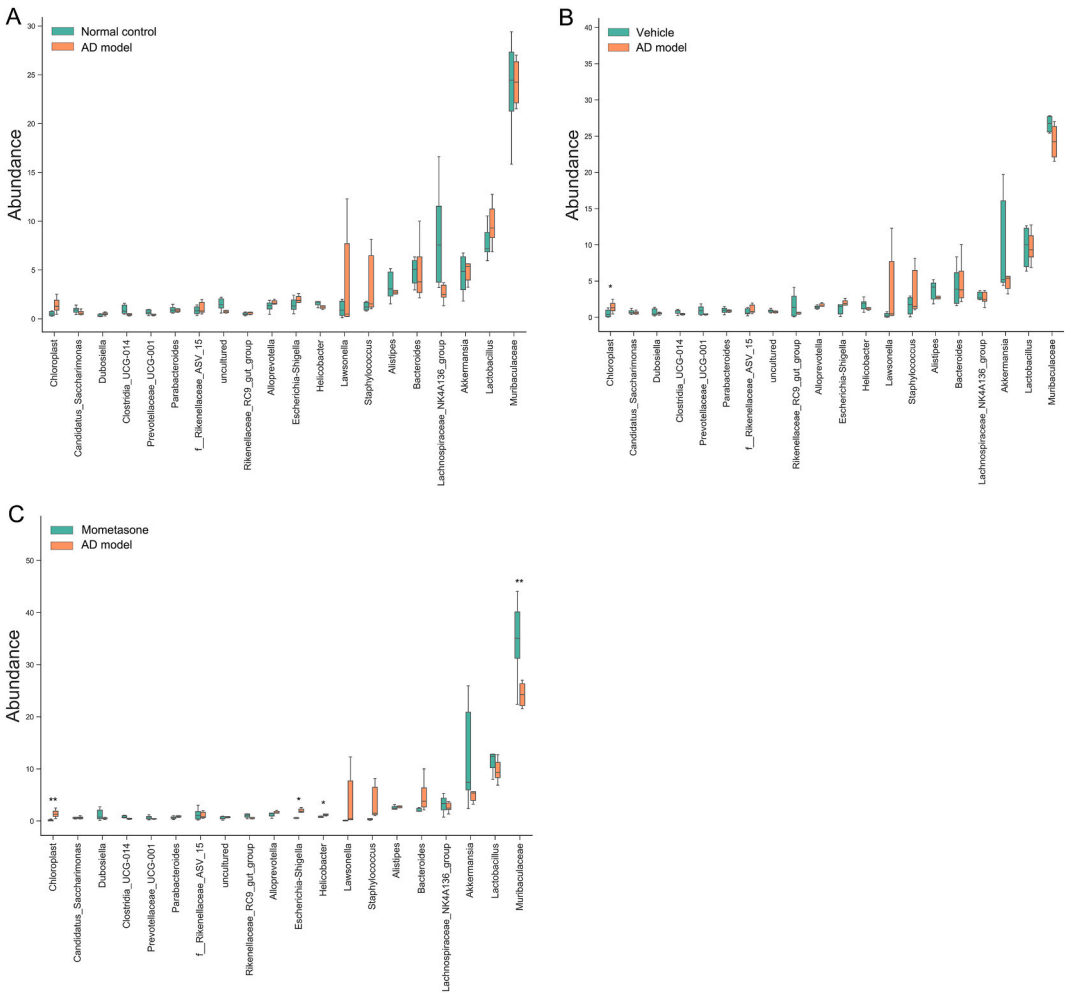

Fig. 6. Comparison of the relative abundance of the dominant microbiota species in mice skins from normal control, vehicle, AD model and Mometasone groups. (A) Normal control group vs. AD group. (B) AD group vs. Vehicle group. (C) AD group vs. Mometasone group. $^{*}P < 0.05$, $^{**}P < 0.01$. The differences in the relative abundance of the dominant microbiota species between two groups were analyzed using the *t*-test test.

bacteria such as *Muribaculaceae* and *Clostridia_UCG-014* [42]. Regarding *Lachnospiraceae*, their anti-inflammatory and immunomodulating effects on the human gut have been reported [43]. As the main producer of anti-inflammatory short-chain fatty acids (SCFAs), *Lachnospiraceae* might improve immune dysfunction in the pathogenesis of chronic spontaneous urticaria [44]. In this study, the relative abundance of *Muribaculaceae*, *Helicobacter*, *Lachnospiraceae_NK4A136_group*, *Prevotellaceae_UCG-001*, and *Clostridia_UCG-014* was decreased in the AD model but increased by CSZYRG treatment. These alterations suggest that the beneficial effects by CSZYRG might be correlated to these bacterial species.

Recent findings show the critical role that dysbiosis of the skin microbiota plays in exacerbating symptoms of AD and point to novel treatment approaches centered on the restoration of microbial balance [11]. The skin of AD patients is characterized by microbial dysbiosis, with a reduction of microbial diversity and overrepresentation of pathogenic *Staphylococcus aureus* [45,46]. Numerous microbes have also been reported to modulate host response through communication with keratinocytes, specialized immune cells, and adipocytes to improve skin health and barrier function [45,47]. Our study contributes to the evidence by demonstrating the potential of a traditional Chinese herbal medicine ointment to modulate skin microbiota and alleviate AD symptoms in a mouse model, offering an alternative to conventional treatments. However, our findings come with limitations, including a small sample size that may affect generalizability and the AD induction localized to the ears. This limitation might not fully reflect the disease's systemic nature or the skin microbiota's variability. These aspects highlight the pressing need for future research with expanded models and larger sample sizes to further validate our results and explore their applicability to human AD treatment, emphasizing the importance of integrating microbiota-focused strategies in clinical management. Besides, our data imply that CSZYRG regulates skin microbiota abundance and reduces inflammation-related variables to treat AD, however, the mechanisms are yet unknown. In addition, the extent to which topical application of CSZYRG affects the development of microbiome composition and structure at other anatomical sites is unknown. Our findings suggest that CSZYRG modulates dominant microbiota and reduces pro-inflammatory cytokines. Further

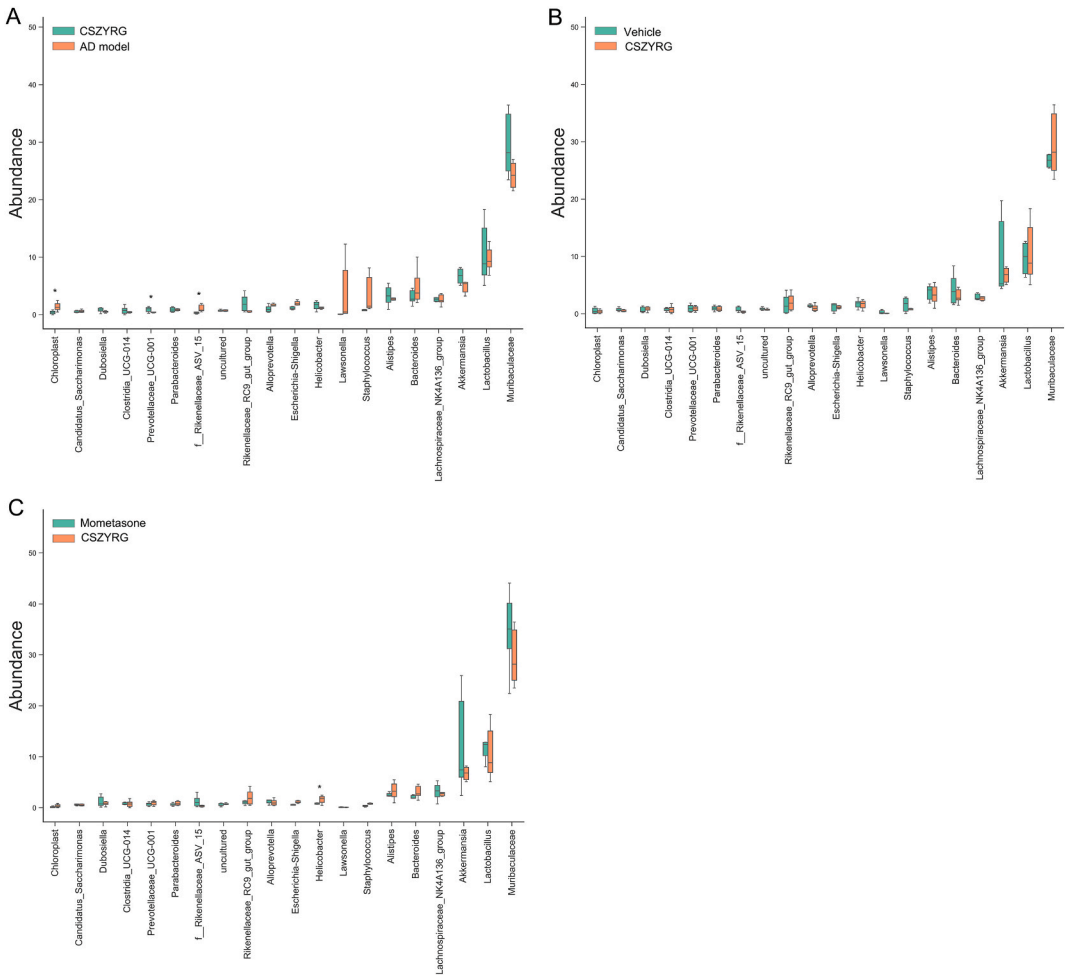

Fig. 7. Comparison of the relative abundance of the dominant microbiota species in mice skins from vehicle, AD model, Mometasone and CSZYRG groups. (A) AD group vs. CSZYRG group. (B) Vehicle group vs. CSZYRG group. (C) CSZYRG group vs. Mometasone group. $^{*}P < 0.05$, $^{**}P < 0.01$. The differences in the relative abundance of the dominant microbiota species between two groups were analyzed using the *t*-test test.

experimental research is required to prove that these microbial alterations cause AD's inflammatory response reduction. Further studies should delve into these complicated connections, maybe using skin microbial removal or transplantation to determine how microbial makeup affects AD-related inflammatory pathways. Such research will confirm CSZYRG's therapy efficacy and help us understand the microbiome's impact on skin health.

In summary, this study shows that CSZYRG can effectively reduce AD clinical manifestations and ameliorate skin lesions and inflammation. It may be related to the recovered relative abundance of *Staphylococcus*, *Muribaculaceae*, *Helicobacter*, *Lachnospiraceae_NK4A136_group*, *Prevotellaceae_UCG-001*, and *Clostridia_UCG-014* in AD mouse skin. This study provides new mechanism ideas for AD treatment by CSZYRG and a new theoretical basis for the clinical treatment of AD.

Ethics approval and consent to participate

All procedures have been approved by the Ethics Committee of Hunan Experimental Animal Center (Approval number: IACUC-2021(5)070).

Data availability

The data supporting this study's findings are available from the corresponding author upon reasonable request.

Funding

This study was supported by Science and Technology Innovation Leading Plan of High-tech Industry of Hunan Province

Table 4
Pairwise comparison of relative median abundance of the skin dominant microbiota between two groups.

Genus	AD model/Normal control	AD model/ Vehicle	AD model/ Mometasone	AD model/ CSZYRG	CSZYRG/ Vehicle	CSZYRG/ Mometasone
Akkermansia	Up 0.823630	Up 0.207657	Down 0.144674	Down 0.260632	Up 0.894022	Down 0.775175
Muribaculaceae	Down 0.823630	Down 0.158906	Down 0.010343**	Down 0.081519	Up 0.434870	Down 0.565056
Helicobacter	Down 0.169459	Down 0.216725	Up 0.033121*	Down 0.370276	Down 0.766307	Up 0.043445*
f_Rikenellaceae_ASV_15	Down 0.455878	Up 0.311159	Down 0.805050	Up 0.049081*	Down 0.206611	Down 0.115636
Parabacteroides	Down 0.993596	Down 0.994404	Up 0.085844	Up 0.732125	Down 0.767186	Up 0.238737
Lachnospiraceae_NK4A136_group	Down 0.079067	Down 0.728506	Down 0.811777	Down 0.751222	Up 0.981501	Down 0.929076
uncultured	Down 0.223287	Down 0.682818	Up 0.329956	Up 0.264159	Down 0.141698	Up 0.902074
Prevotellaceae_UCG-001	Down 0.210353	Down 0.109111	Down 0.175606	Down 0.049781*	Up 0.895600	Up 0.413571
Lactobacillus	Up 0.137092	Down 0.665136	Down 0.268821	Up 0.675446	Down 0.961712	Down 0.344305
Dubosiella	Up 0.085111	Up 0.367409	Down 0.164967	Down 0.116514	Up 0.900401	Up 0.562673
Bacteroides	Down 0.967436	Down 0.744805	Up 0.062745	Up 0.394901	Down 0.594957	Up 0.165296
Rikenellaceae_RC9_gut_group	Up 0.329923	Down 0.231408	Down 0.288723	Down 0.075889	Up 0.717363	Up 0.148012
Lawsonella	Down 0.519450	Up 0.142162	Up 0.299085	Up 0.132388	Down 0.575440	Up 0.398970
Staphylococcus	Up 0.489010	Down 0.346159	Up 0.060876	Up 0.692005	Down 0.482500	Up 0.332253
Candidatus_Saccharimonas	Down 0.145728	Down 0.539571	Up 0.888811	Up 0.394069	Down 0.189068	Down 0.453057
Clostridia_UCG-014	Down 0.124923	Down 0.083363	Down 0.118285	Down 0.330564	Down 0.990915	Up 0.881786
Chloroplast	Up 0.117845	Up 0.049144*	Up 0.002735**	Up 0.013816*	Down 0.571722	Up 0.130621
Alistipes	Down 0.293637	Down 0.161028	Up 0.467336	Down 0.451954	Down 0.678023	Up 0.249474
Escherichia-Shigella	Up 0.353783	Up 0.869465	Up 0.020397*	Up 0.085658	Down 0.462257	Up 0.162790
Alloprevotella	Up 0.224432	Up 0.209724	Up 0.369817	Up 0.068745	Down 0.217990	Down 0.401833

*$p < 0.05$, **$p < 0.01$.

(2020SK2023), the First-level Discipline Open Fund Project of Nursing in Hunan University of Chinese Medicine (2020HLX02), Henan Province Science and Technology Research Project (212102311120 and 162102310179) and Top TCM Talents Training Project of Henan Province (Yuwei TCM Letter [2021] No. 15).

CRediT authorship contribution statement

Bijun Zeng: Writing – review & editing, Writing – original draft, Conceptualization. **Xuewei Liu:** Investigation. **Yi Zhou:** Investigation. **Gutao Cui:** Software, Data curation. **Lili An:** Software, Data curation. **Zhibo Yang:** Writing – review & editing, Project administration, Funding acquisition, Conceptualization.

Declaration of competing interest

The authors declare that they have no known competing financial interests or personal relationships that could have appeared to influence the work reported in this paper.

Acknowledgements

None.

Appendix A. Supplementary data

Supplementary data to this article can be found online at https://doi.org/10.1016/j.heliyon.2024.e33240.

References

[1] S. Feng, G. Song, L. Liu, W. Liu, G. Liang, Z. Song, Allergen-specific immunotherapy induces monocyte-derived dendritic cells but attenuates their maturation and cytokine production in the lesional skin of an atopic dermatitis mouse model, J. Dermatol. 49 (12) (2022) 1310–1319.
[2] L. Liu, G. Song, Z. Song, Intrinsic atopic dermatitis and extrinsic atopic dermatitis: similarities and differences, Clin. Cosmet. Invest. Dermatol. (2022) 2621–2628.
[3] W. Frazier, N. Bhardwaj, Atopic dermatitis: Diagnosis and treatment, Am. Fam. Physician 101 (10) (2020) 590–598.
[4] L.F. Eichenfield, W.L. Tom, S.L. Chamlin, S.R. Feldman, J.M. Hanifin, E.L. Simpson, et al., Guidelines of care for the management of atopic dermatitis: section 1. Diagnosis and assessment of atopic dermatitis, J. Am. Acad. Dermatol. 70 (2) (2014) 338–351.
[5] J.I. Silverberg, E.L. Simpson, Association between severe eczema in children and multiple comorbid conditions and increased healthcare utilization, Pediatr. Allergy Immunol. 24 (5) (2013) 476–486.
[6] L. Serrano, K.R. Patel, J.I. Silverberg, Association between atopic dermatitis and extracutaneous bacterial and mycobacterial infections: a systematic review and meta-analysis, J. Am. Acad. Dermatol. 80 (4) (2019) 904–912.
[7] J.A. Ellison, L. Patel, D.W. Ray, T.J. David, P.E. Clayton, Hypothalamic-pituitary-adrenal function and glucocorticoid sensitivity in atopic dermatitis, Pediatrics 105 (4 Pt 1) (2000) 794–799.
[8] C. DiNicola, A. Kekevian, C. Chang, Integrative medicine as adjunct therapy in the treatment of atopic dermatitis–the role of traditional Chinese medicine, dietary supplements, and other modalities, Clin. Rev. Allergy Immunol. 44 (3) (2013) 242–253.
[9] SpgoCAGftToDDbpC. Medicines, L. Li, Y. Li, Guidelines for clinical application of proprietary traditional Chinese medicines in the treatment of eczema (2020), Chin. J. Integr. Med. 41 (2) (2021) 10.
[10] J. Lee, L. Bielory, Complementary and alternative interventions in atopic dermatitis, Immunol. Allergy Clin. 30 (3) (2010) 411–424.
[11] D. Hrestak, M. Matijašić, H. Čipčić Paljetak, D. Ledić Drvar, S. Ljubojević Hadžavdić, M. Perić, Skin microbiota in atopic dermatitis, Int. J. Mol. Sci. 23 (7) (2022).
[12] L. Liu, K. Qiu, Efficacy of Chushi and Zhiyang Ointment combined with levocetirizine in the treatment of chronic perianal eczema and its impact on patients' quality of life, Journal of Clinical Medicine in Practice 21 (13) (2017) 182–184.
[13] G. Tao, Observation on the effect of 60 cases of chronic eczema treated with Chushi Zhiyang ointment combined with mometasone furoate cream, Medical Journal of Communications 25 (6) (2011) 602–604.
[14] X. Chen, C. Zhu, Y. Zhang, N. Yang, H. Shi, W. Yang, et al., Antipruritic effect of Ethyl acetate Extract from in mice with 2,4-Dinitrofluorobenzene-induced atopic dermatitis, Evid. base Compl. Alternative Med. : ECAM. 2020 (2020) 6981386.
[15] S. Park, D.S. Kim, S. Kang, B.K. Shin, Synergistic topical application of salt-processed Phellodendron amurense and Sanguisorba officinalis Linne alleviates atopic dermatitis symptoms by reducing levels of immunoglobulin E and pro-inflammatory cytokines in NC/Nga mice, Mol. Med. Rep. 12 (5) (2015) 7657–7664.
[16] B.-M. Choi, G.-S. Oh, J.W. Lee, J.Y. Mok, D.K. Kim, S.-I. Jeong, et al., Prenylated chalcone from Sophora flavescens suppresses Th2 chemokine expression induced by cytokines via heme oxygenase-1 in human keratinocytes, Arch Pharm. Res. (Seoul) 33 (5) (2010) 753–760.
[17] A.L. Byrd, Y. Belkaid, J.A. Segre, The human skin microbiome, Nat. Rev. Microbiol. 16 (3) (2018) 143–155.
[18] A.S. Paller, H.H. Kong, P. Seed, S. Naik, T.C. Scharschmidt, R.L. Gallo, et al., The microbiome in patients with atopic dermatitis, J. Allergy Clin. Immunol. 143 (1) (2019) 26–35.
[19] T. Nakatsuji, T.H. Chen, S. Narala, K.A. Chun, A.M. Two, T. Yun, et al., Antimicrobials from human skin commensal bacteria protect against and are deficient in atopic dermatitis, Sci. Transl. Med. 9 (378) (2017).
[20] I.A. Myles, N.J. Earland, E.D. Anderson, I.N. Moore, M.D. Kieh, K.W. Williams, et al., First-in-human topical microbiome transplantation with Roseomonas mucosa for atopic dermatitis, JCI insight 3 (9) (2018) e120608.
[21] J. Hanifin, M. Thurston, M. Omoto, R. Cherill, S. Tofte, M. Graeber, et al., The eczema area and severity index (EASI): assessment of reliability in atopic dermatitis 10 (1) (2001) 11–18.
[22] J. Yi, L. Li, Z.J. Yin, Y.Y. Quan, R.R. Tan, S.L. Chen, et al., Polypeptide from Moschus suppresses Lipopolysaccharide-induced inflammation by inhibiting NF-κ B-ROS/NLRP3 pathway, Chin. J. Integr. Med. 29 (10) (2023) 895–904.
[23] K. Findley, J. Oh, J. Yang, S. Conlan, C. Deming, J.A. Meyer, et al., Topographic diversity of fungal and bacterial communities in human skin, Nature 498 (7454) (2013) 367–370.
[24] E.K. Costello, C.L. Lauber, M. Hamady, N. Fierer, J.I. Gordon, R. Knight, Bacterial community variation in human body habitats across space and time, Science (New York, NY) 326 (5960) (2009) 1694–1697.
[25] E.A. Grice, H.H. Kong, S. Conlan, C.B. Deming, J. Davis, A.C. Young, et al., Topographical and temporal diversity of the human skin microbiome, Science (New York, NY) 324 (5931) (2009) 1190–1192.
[26] H.H. Kong, Segre JajjoID, The molecular revolution in cutaneous biology: investigating the skin microbiome 137 (5) (2017) e119–e122.
[27] J. Oh, A.L. Byrd, M. Park, H.H. Kong, J.A. Segre, Temporal Stability of the human skin microbiome, Cell 165 (4) (2016) 854–866.
[28] P.C. Zhongkui Huang, Wei Wennan, Effect of Dehumidifying and Relieving itching ointment on atopic dermatitis, Modern journal of integrated traditional chinese and western medicine 19 (21) (2010) 2.
[29] Xu YC. Binfei, Daxing Wu, Effect of Dehumidification antipruritic ointment on immune function and serum levels of TNF-α,IL-4 and IL-6 in children with atopic dermatitis, Modern medicine and health research 4 (12) (2020) 65–67.
[30] N. Fischer, G.L. Darmstadt, K.M. Shahunja, J.M. Crowther, L. Kendall, R.A. Gibson, et al., Topical emollient therapy with sunflower seed oil alters the skin microbiota of young children with severe acute malnutrition in Bangladesh: a randomised, controlled study, J Glob Health 11 (2021) 04047.
[31] W. Lu, Y. Deng, Z. Fang, Q. Zhai, S. Cui, J. Zhao, et al., Potential role of Probiotics in ameliorating psoriasis by modulating gut microbiota in Imiquimod-induced psoriasis-like mice, Nutrients 13 (6) (2021).
[32] R. Liu, C. Peng, D. Jing, Y. Xiao, W. Zhu, S. Zhao, et al., Biomarkers of gut microbiota in chronic spontaneous urticaria and Symptomatic Dermographism, Front. Cell. Infect. Microbiol. 11 (2021).
[33] L. Dong, H. Du, M. Zhang, H. Xu, X. Pu, Q. Chen, et al., Anti-inflammatory effect of Rhein on ulcerative colitis via inhibiting PI3K/Akt/mTOR signaling pathway and regulating gut microbiota, Phytother Res. 36 (5) (2022) 2081–2094.
[34] I.H. Galadari, M.O. Sheriff, The role of Helicobacter pylori in urticaria and atopic dermatitis, Skinmed 5 (4) (2006) 172–176.
[35] C. Guarneri, M. Ceccarelli, L. Rinaldi, B. Cacopardo, G. Nunnari, F. Guarneri, Helicobacter pylori and skin disorders: a comprehensive review of the available literature, Eur. Rev. Med. Pharmacol. Sci. 24 (23) (2020) 12267–12287.
[36] Q. Xue, X. Li, Y. Li, J. Xu, Z. Wu, J. Wang, Dialogue between gastrointestinal tract and skin: new insights into the Helicobacter pylori and atopic dermatitis, Helicobacter 26 (2) (2021) e12771.
[37] K. Hou, Z.-X. Wu, X.-Y. Chen, J.-Q. Wang, D. Zhang, C. Xiao, et al., Microbiota in health and diseases, Signal Transduct. Targeted Ther. 7 (1) (2022) 135.
[38] E.H. van den Bogaard, P.M. Elias, E. Goleva, E. Berdyshev, J.P.H. Smits, S.G. Danby, et al., Targeting skin barrier function in atopic dermatitis, J. Allergy Clin. Immunol. Pract. 11 (5) (2023) 1335–1346.
[39] Y. Liu, S. Wang, W. Dai, Y. Liang, C. Shen, Y. Li, et al., Distinct skin microbiota Imbalance and responses to clinical treatment in children with atopic dermatitis, Front. Cell. Infect. Microbiol. 10 (2020) 336.
[40] I. Lagkouvardos, T.R. Lesker, T.C.A. Hitch, E.J.C. Gálvez, N. Smit, K. Neuhaus, et al., Sequence and cultivation study of Muribaculaceae reveals novel species, host preference, and functional potential of this yet undescribed family, Microbiome 7 (1) (2019) 28.
[41] H. Liang, H. Song, X. Zhang, G. Song, Y. Wang, X. Ding, et al., Metformin attenuated sepsis-related liver injury by modulating gut microbiota, Emerg Microbes Infect 11 (1) (2022) 815–828.

[42] Y. Liu, M. Zhou, M. Yang, C. Jin, Y. Song, J. Chen, et al., Pulsatilla chinensis saponins ameliorate inflammation and DSS-induced ulcerative colitis in Rats by regulating the composition and diversity of Intestinal flora, Front. Cell. Infect. Microbiol. 11 (2021) 728929.
[43] R. Abdugheni, W.-Z. Wang, Y.-J. Wang, M.-X. Du, F.-L. Liu, N. Zhou, et al., Metabolite profiling of human-originated Lachnospiraceae at the strain level, iMeta 1 (4) (2022) e58.
[44] D. Cesic, L. Lugovic Mihic, P. Ozretic, I. Lojkic, M. Buljan, M. Situm, et al., Association of gut Lachnospiraceae and chronic spontaneous urticaria, Life 13 (6) (2023).
[45] L.F. Koh, R.Y. Ong, J.E. Common, Skin microbiome of atopic dermatitis, Allergol. Int. 71 (1) (2022) 31–39.
[46] S.M. Edslev, T. Agner, P.S. Andersen, Skin microbiome in atopic dermatitis, Acta Derm. Venereol. 100 (12) (2020) adv00164.
[47] C.S. Moniaga, M. Tominaga, K. Takamori, An altered skin and gut microbiota are involved in the modulation of itch in atopic dermatitis, Cells 11 (23) (2022) 3930.